Multi-Objective Optimal SVC Installation for Power System Loading Margin Improvement

Ya-Chin Chang, *Member, IEEE*

***Abstract*—Proper installation of flexible ac transmission systems (FACTS) in existing transmission networks can improve transmission system loading margin (LM) to a certain degree and reduce network expansion cost. In the paper, under each contingency with high risk index (RI) value, the modal analysis (MA) technique is used to determine which buses need static var compensator (SVC) installation, and with maximum LM and minimum SVC installation cost composed into the multi-objective function the optimal LM enhancement problem is formulated as a multi-objective optimization problem (MOP) and solved by using the fitness sharing multi-objective particle swarm optimization (MOPSO) algorithm for a Pareto front set. In the Pareto front set for each considered contingency, the solution with the biggest performance index value is determined for SVC installation. Finally, an SVC installation scheme derived from the union of the SVC installations for all considered contingencies is recommended for LM enhancement. The proposed method is validated on the IEEE 24-bus reliability test system (RTS) and a practical power system.**

***Index Terms*—Continuation power flow, loading margin, modal analysis, Pareto front, risk index, static voltage stability.**

I. Introduction

UNDER urgency to diminish the harms from environmental deterioration, one of the recently focused researches in the power industry is to make the existing transmission networks sufficiently utilize their capability in power transfer [1]–[3]. Through detailed studies, voltage instability was found to be the main factor responsible for several blackout events in the recent years [4]. As an index to indicate the level of static voltage stability of a transmission system, the loading margin (LM) or voltage stability margin (VSM), representing the maximum power that can be transferred between generators and loads before voltage collapse point achieved is generally measured in system planning [5], [6].

The optimal flexible ac transmission systems (FACTS) installation had been researched and discussed widely and several strategies were proposed. In general, the studies are oriented towards technical, economic, or both concerns. In technical concerns, the method proposed in [3] practically installed different types of FACTS devices on different locations to identify the increase of LM. While in [7], a two-stage SVC installation method is proposed. In stage one, LM is increased on a step-by-step basis and, in each step, to provide sufficient reactive power from an SVC installation, the location and its capacity are determined by using a genetic algorithm (GA), and, in stage two, under different contingencies the control signals to the SVC installation are determined based on various stability indices. The method proposed in [8] used GA to determine the locations and capacities for the respective installations of various types of FACTS devices for LM enhancement. While in [9], modal analysis (MA) technique and a guaranteed convergence particle swarm optimization (GCPSO) algorithm are used to determine the locations for SVC installation and the capacities to enhance LM. With the compensation of SVC, TCSC, and UPFC installations, in [10], the singular value/eigenvalue decomposition analysis of the load-flow Jacobian and the controllability characteristics of an equivalent state model are used to study the voltage instability phenomenon as well as to assess the potential for small-signal voltage stability improvement. Considering $\mathrm{N}-1$ contingencies, in [11], tangent vector technique and reactive power sensitivity index were adopted as reference indices to point out the locations suitable for installations of the parallel and series FACTS devices. As specific contingencies are identified to be the main factors that result in voltage instability, [12] expressed $\mathrm{N}-1$ line outages with stochastic model and used MA to expect the total participation in all critical modes (TPCM) index value for each bus. The bus with the biggest TPCM index value is selected for a STATCOM installation.

On the other hand, in economic concerns, the total FACTS installation and generation costs were taken as the objective function in [13] and [14], and GA was used to make the decision where to install FACTS devices. The method proposed in [15], comprised of the tabu search (TS) and a nonlinear programming method, was used to optimize the FACTS devices investment and recovery. While the method developed in [16] with the proposed performance indices of real power flows was used to seek the optimal locations for FACTS installation. Under the existing FACTS devices installed, in [17], the minimum generation cost-based OPF was solved using the proposed hybrid of TS and simulated annealing (SA) algorithm. While in [18], an optimal approach comprised of CPF and OPF techniques for UPFC installation was proposed to minimize the total generation and installation cost.

Dealing with both concerns simultaneously in the LM enhancement problem for deriving optimal FACTS installation, in [19], the proposed method linearly composed voltage security, system loss, capacities for STATCOM installation and LM

Manuscript received May 20, 2011; revised September 25, 2011; accepted November 07, 2011. Date of publication December 19, 2011; date of current version April 18, 2012. This work was supported by the National Science Council under project number NSC 98-2221-E-230-017. Paper no. TPWRS-00473-2011.

The author is with the Department of Electrical Engineering, Cheng Shiu University, Kaohsiung 833, Taiwan (e-mail: ycchang@mail.csu.edu.tw).

Color versions of one or more of the figures in this paper are available online at http://ieeexplore.ieee.org.

Digital Object Identifier 10.1109/TPWRS.2011.2176517

0885-8950/$26.00 © 2011 IEEE

into a single-objective function, which was solved by using a PSO algorithm. While in [20] and [21], a single objective function was linearly composed of the installation costs for various types of FACTS devices (UPFC, TCSC, SVC), system securities, loss and voltage stability indices. The problem was solved by PSO in [20] and GA in [21]. Besides, to possibly reveal the variety of solutions, the optimal SVC installation problem for LM enhancement is formulated as an MOP. Reference [22] applied a multi-objective genetic algorithm (MOGA) to the combinatorial optimization problem with the multi-objective function composed of minimum FACTS installation cost and allowable system security limits. The results obtained to release the threats from low voltage and line congestion include the types of FACTS devices used, the installation locations and capacities. While in [23], the minimum generation costs and allowable system security limits are involved in the multi-objective function, and a bacterial swarming algorithm (BSA) is used to determine the installation locations and capacities for various types of FACTS devices (TCSC, TCPST, TCVR, SVC). The method proposed in [24] composed maximum LM, minimum system loss and voltage deviations at PQ buses into the multi-objective function, and an MOPSO method was used to solve for the locations and capacities for one SVC and one TCSC installations.

From previous reviews, a FACTS installation problem can adopt linearization approaches, or methods with more flexibility including heuristic models and evolutional algorithms. In the paper, both concerns are dealt with at one time. First the risk index (RI) is used to assess the risk level caused by each contingency, and the contingencies with RI values bigger than the specified are considered for SVC installation. Then, under each considered contingency, MA technique is used to determine which buses need SVC installation, and the LM enhancement problem to determine the capacity of each SVC installation and generation pattern [6] is formulated as an MOP with maximum LM and minimum SVC installation cost involved in the multi-objective function. The fitness sharing MOPSO algorithm is used to solve for a Pareto front set from the MOP for each considered contingency [25], [26]. Also, the performance index, defined as the ratio of the LM to the installation cost, is used to determine a solution from the Pareto front set with LM bigger than or equal to the required LM. Finally, the locations and capacities for SVC installation derived from the union of the solutions for all considered contingencies are taken as the optimal SVC installation for LM enhancement, resulting in that the static voltage stability under each contingency can be maintained for allowable load increases.

II. Problem Formulation

A. Multi-Objective Optimization Problems

When trying to solve an MOP, not only trying to look for one single solution but a set of trade-off solutions is the target of the solution algorithm and the one that will be chosen will depend on the needs of the decision maker. An MOP can be defined as

$$\begin{aligned} Min \quad & f(u) = [f_1(u), f_2(u), \ldots, f_k(u)]^{\mathrm{T}} \\ \text{s.t.} \quad & h(u) = 0 \\ & g(u) \le 0 \end{aligned} \tag{1}$$

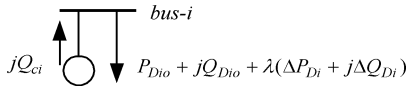

Fig. 1. PQ bus with an SVC installation.

where multi-objective function f includes k ($k \ge 2$) objective functions, constraints $h(u)$ and $g(u)$ are equality and inequality functions, and u is control variables.

In order to optimize the vector function, the concepts tied to an MOP called "domination" and "nondomination" are defined as [25]: *1) Solution u_1 is said to dominate solution u_2, if and only if u_1 is not worse than u_2 in all objectives and u_1 is strictly better than u_2 in at least one objective. 2) Among a set of solutions P, the nondominated set of solutions P' are those that are not dominated by any member of the set P.*

If within the definition the set of solution P is replaced by the feasible search space F ($P = F$), then the set of solutions in P' will be what is called Pareto-optimal set or Pareto front.

B. Problem Formulation for Loading Margin Enhancement

Let Q_{ci} be a regulable reactive power provided by the SVC at bus i and its range is set to: $-\overline{Q}_c \le Q_{ci} \le \overline{Q}_c$. Fig. 1 shows the equivalent injection for a PQ bus with an SVC installation. Employing CPF technique to formulate the LM enhancement problem and letting λ, $\lambda \ge 0$, be the loading factor, $\lambda = 0$ for base load, the real and reactive power balance equations on bus i are expressed as

$$\sum_{j=1}^{n} P_{ij} + P_{io} - \lambda(\Delta P_{Gi} - \Delta P_{Di}) = 0 \tag{2}$$

$$\sum_{j=1}^{n} Q_{ij} + Q_{io} + \lambda(\Delta Q_{Di}) + Q_{ci} = 0. \tag{3}$$

$P_{io} = -P_{Gio} + P_{Dio}$ and $Q_{io} = -Q_{Gio} + Q_{Dio}$ are the base real and reactive power injections for the generator and load at bus i, and ΔP_{Gi}, and ΔP_{Di}, and ΔQ_{Di} are the generation increment and loading level. In the paper, the loading level is set to the base load such that the power factors are fixed as load changed with λ. The real and reactive power flows are

$$P_{ij} = V_i^2 G_{ij} - V_i V_j (G_{ij} \cos\delta_{ij} + B_{ij} \sin\delta_{ij}) \tag{4}$$

$$\begin{aligned} Q_{ij} = & -V_i^2 (B_{ij} + B_{sh}) \\ & - V_i V_j (G_{ij} \sin\delta_{ij} - B_{ij} \cos\delta_{ij}). \end{aligned} \tag{5}$$

The power flow balance (2) and (3) are expressed in an equality functional vector as follows:

$$h(x, u, \lambda) = 0 \tag{6}$$

where system variables vector $x = [\boldsymbol{\theta} \quad \mathbf{V}]^{\mathrm{T}}$ including bus voltage magnitudes and phase angles, and control variables vector $u = [\mathbf{\Delta P_G} \quad \mathbf{Q_C}]^{\mathrm{T}}$ including the generation increments (or generation pattern) and reactive power injections $\mathbf{Q_C}$ of all SVC installations. Also, the inequality constraints that should be satisfied with include the limits of real and reactive

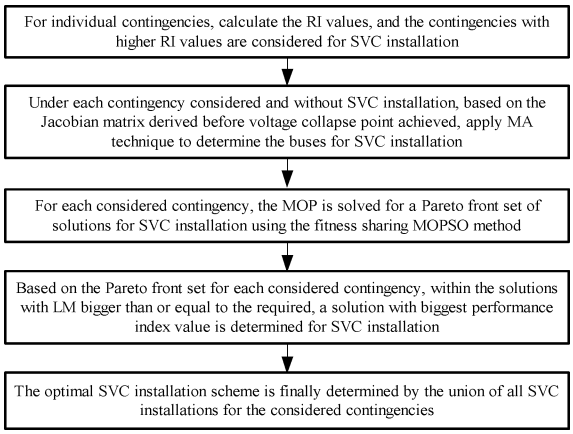

Fig. 2. Proposed LM enhancement strategy.

power generations, and the capacities of existing control devices (AVR, SC, OLTC) and SVC installations, expressed in an inequality functional vector as follows:

$$g(x, u, \lambda) \leq 0. \tag{7}$$

Based on specific control variables values, the maximum loading factor λ^* can be calculated using CPF process and the LM is derived as $\lambda^* \sum_{\forall i} \Delta P_{Di}$. The objective functions include maximum system LM (represented as λ), denoted as f_1, and minimum SVC installation cost, denoted as f_2. The two objective functions are integrated into a multi-objective function, expressed as a functional vector in the following:

$$f = [f_1\ f_2]^{\mathrm{T}}. \tag{8}$$

If five years is the lifetime for an SVC installation, the operating cost (US$/h) for all SVC installations is [27]

$$f_2 = \frac{\sum_{\forall i} (0.0003 Q_{ci}^2 - 0.3051 Q_{ci} + 127.38) 10^5 \cdot Q_{ci}}{(5 \cdot 8760)}. \tag{9}$$

From (2) to (9), the LM enhancement problem with SVC installation is formulated as an MOP as follows:

$$\begin{aligned} Min \quad & f \\ s.t. \quad & h(x, u, \lambda) = 0 \\ & g(x, u, \lambda) \leq 0 \\ & 0 \leq \lambda. \end{aligned} \tag{10}$$

In the paper, the MOP for each considered contingency is solved by using the fitness sharing MOPSO algorithm, and from the obtained Pareto front set, a solution with $\lambda^* \geq \lambda_{req}$ and maximum performance index value f_1/f_2 is determined for SVC installation, where λ_{req} represents the required LM.

III. MOP-Based SVC Installation Strategy

The LM enhancement strategy for SVC installation proposed in the paper is shown in Fig. 2. The key approaches used to realize the strategy are introduced as follows.

A. Outage Risk Index

In order to maintain system operating at static voltage stability under each outage, transmission systems need sufficient LM to avoid voltage instability while accommodating more power transfer. Since contingency events inevitably result in LM decrease, those contingencies with bigger failure probability and resulting in more LM decrease will have bigger RI values, namely requiring reactive power compensation. Under normal state and without SVC installation, the system LM represented as a loading factor is assumed to be λ^*_{nor}. When contingency E_i happens, the LM becomes $\lambda^*_{E_i}$, resulting in a decreased LM expressed as $\Delta\lambda_{E_i} = \lambda^*_{nor} - \lambda^*_{E_i}$. The RI value under contingency E_i is calculated from

$$Risk(E_i) = P_r(E_i) \times \Delta\lambda_{E_i} \tag{11}$$

where $P_r(E_i)$ is the failure probability of contingency E_i. The failure rate of the contingency is expressed as α_{E_i} which can be obtained from the power supply department. It is assumed that the contingency events are independent, and under a contingency, during the period of voltage instability resulted from demand increase, the component is assumed not to be repairable. The failure rate is converted to the failure probability by a Poisson distribution [28]:

$$P_r(E_i) = 1 + \frac{e^{-\alpha_{E_i} \mathrm{T}_r} - 1}{\alpha_{E_i} T_r} \tag{12}$$

where $P_r(E_i)$ is the average outage probability of contingency E_i in a defined time interval T_r (one year).

B. Modal Analysis

Reactive power is the most important factor to voltage stability. From the expectation of the impact level on voltage stability from load increase, the signals on which buses the reactive power compensation is necessary for maintaining enough system LM can be obtained. For each contingency, using the Jacobian matrix obtained close to the voltage collapse point during the computation for system LM, the derived first order system equation is shown in the following:

$$\begin{bmatrix} \Delta P \\ \Delta Q \end{bmatrix} = \begin{bmatrix} J_{P\theta} & J_{PV} \\ J_{Q\theta} & J_{QV} \end{bmatrix} \begin{bmatrix} \Delta\theta \\ \Delta V \end{bmatrix} \tag{13}$$

where vectors ΔP and ΔQ, and vectors $\Delta\theta$ and ΔV, are the changes of bus real and reactive powers, and voltage magnitudes and angles, respectively. To highlight the relationship between ΔQ and ΔV, by neglecting the effect of real power changes, (13) can be simplified to [12]

$$\Delta Q = \left(J_{QV} - J_{Q\theta} \cdot J_{P\theta}^{-1} \cdot J_{PV}\right) \cdot \Delta V. \tag{14}$$

Rearranging (14) obtains

$$\Delta V = J_R^{-1} \Delta Q \tag{15}$$

where $J_R = (J_{QV} - J_{Q\theta} \cdot J_{P\theta}^{-1} \cdot J_{PV})$ called the simplified Jacobian matrix which can be used to describe the relationships between the changes of bus voltages and reactive powers. Assume

$$J_R = \xi \Lambda \eta. \tag{16}$$

In (16), ξ and η are the orthornormal matrices composed of the right and left singular vectors, respectively, and Λ the system diagonal singular values matrix; $\xi^{-1} = \eta$. From (15) and (16), the variations of bus voltages can be expressed as

$$\Delta V = \xi \Lambda^{-1} \eta \Delta Q \tag{17}$$

and

$$v = \Lambda^{-1} q \tag{18}$$

where $v = \eta \Delta V$ is the vector of modal voltage variations and $q = \eta \Delta Q$ the vector of modal reactive power variations. From (18), the ith modal voltage variation due to the changes of bus reactive powers can be obtained with

$$v_i = \frac{1}{\sigma_i} q_i. \tag{19}$$

It can be seen from (19) that the smaller the singular value σ_i of the ith modal is, the bigger the modal voltage will be, resulting in higher risk to voltage instability. When there is reactive power change at bus j, the associated ith modal voltage can be derived from

$$v_{ij} = \frac{\eta_{ij}}{\sigma_i} \Delta Q_j = R_{ij} \Delta Q_j. \tag{20}$$

In (20), R_{ij} associates the ith modal voltage with the reactive power change at bus j. The voltage instability contribution factor (CF) is specified as the modal voltage caused by the load change at bus j which can be calculated as

$$CF_j = \sum_{i=1}^{m} R_{ij} \tag{21}$$

where index m is the modal number.

Under each contingency condition, the buses with bigger voltage instability CF are considered for SVC installation.

C. Multi-Objective Optimization Problem Solution Method

In the algorithm, particle position and velocity are updated using the following two equations [9]:

$$X_i(k+1) = X_i(k) + V_i(k+1) \tag{22}$$

$$v_{i,j}(k+1) = w v_{i,j}(k) + c_1 r_{1,j}(pbest_{i,j} - x_{i,j}(k)) + c_2 r_{2,j}(gbest_j - x_{i,j}(k)). \tag{23}$$

$X_i(k)$ and $V_i(k)$ represent the position and velocity of particle i at iteration k. $x_{i,j}$ is the jth entry of $X_i(k)$. $v_{i,j}$ is the jth entry of V_i that denotes the velocity of $X_i(k)$; $0 \le w \le 1$ is an inertia weight determining how much the particle's previous velocity is preserved; c_1 and c_2 are two positive acceleration constants; $r_{1,j}$, $r_{2,j}$ are random numbers sampled from uniform distribution $U(0,1)$; $pbest_i$ and $gbest$ are the personal best position of particle i and the best position in the entire swarm, respectively.

The fitness sharing technique [25] is used to modify the PSO into an MOPSO for solving the MOP described above. The fitness sharing scheme is to distribute a population of particles along a set of resources. When a particle i is sharing resources with other particles, its fitness f_i is degraded proportional to the number and closeness to particles that surround it. If maximum objective is the target of the problem, the fitness sharing for particle i is defined as

$$fs_i = \frac{f_i}{\sum_{k=1}^{NP} sh_i^k}. \tag{24}$$

A bigger fitness sharing represents that the particle is distant from the swarm. On the other hand, while the target is to seek a minimum objective, the fitness sharing is defined as

$$fs_i = f_i \cdot \sum_{k=1}^{NP} sh_i^k \tag{25}$$

where sh_i^k denotes the sharing factor that measures the similarity from particles i to k by a distance function d_i^k. When the particle is averagely more distant from other particles, a smaller sharing factor takes place

$$sh_i^k = \begin{cases} 1 - \left(\frac{d_i^k}{\sigma}\right)^2, & \text{if } d_i^k < \sigma \\ 0, & \text{otherwise} \end{cases} \tag{26}$$

and

$$d_i^k = \sum_j \left(\frac{x_{i,j} - x_{k,j}}{x_j^{\max} - x_j^{\min}} \right)^2 \tag{27}$$

where σ denotes the distance for the particles to remain distant from each other and j indexing variables in particle x. σ is set on a case-by-case basis. A particle with the best fitness sharing will take the position to guide the swarm into the next generation. With the fitness sharing scheme involved in the solution process, the determination of $gbest$ in the traditional PSO algorithm is changed to

$$gbest = \text{the } pbest \text{ of the particle with maximum (or minimum) fitness sharing.}$$

Fig. 3 shows the fitness sharing MOPSO algorithm used to find a Pareto front set of solutions for SVC installation under each considered contingency. The use of PSO technique is to guide the search with help of fitness sharing to spread the particles along the Pareto front. Fitness sharing will help to maintain diversity between solutions, and thus particles within high populated areas in the objective space will be less likely to be followed. In each iteration, the best particles found (those not dominated) will be inserted into an external repository. This repository will help to guide the search for the next generations and maintain a set of not dominated solutions until the end of the run, which form the Pareto front set.

Referring to the LM enhancement strategy proposed in Fig. 2, after the Pareto front set for each considered contingency is derived, within the solutions with $\lambda^* \ge \lambda_{req}$, a solution that has maximum performance index f_1/f_2 value is specified as the SVC installation for the contingency. Finally, the optimal

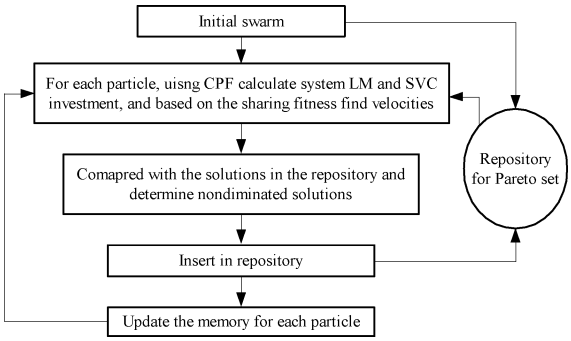

Fig. 3. Fitness sharing MOPSO algorithm.

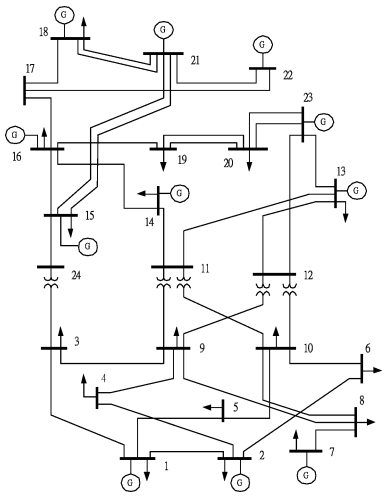

Fig. 4. Modified IEEE 24-bus reliability test system.

SVC installation is resulted from the union of the SVC installations for all considered contingencies. It is conceivable that, compared to the SVC installation for each contingency, the optimal SVC installation would have bigger SVC units number, each SVC installation with bigger or equal capacity.

IV. Test Results and Discussions

A. IEEE 24-Bus RTS

The IEEE 24-bus RTS with bus 13 as the swing bus, 10 PV bus and bus 14 connected with an AVR, and 34 transmission lines, shown in Fig. 4, is used for testing. The data of the transmission lines are shown in Table I, where line failure rates are shown in the last column, for example, that the rate of line 1 outage occurrences per year is 0.24 (Occ./yr). The base load and power supplies with 100 MVA as base are shown in Table II. The base-case load flows are shown in Table III. Letting load increments ΔP_{Di} and ΔQ_{Di} for each PQ bus i equal the base load, thus during LM calculation the power factors for all loads are fixed and the base real power demand equates $\sum_{\forall i} \Delta P_{Di} = 37.05$ p.u.

Under normal state, the transmission system has LM calculated as $\lambda^*_{nor} \sum_{\forall i} \Delta P_{Di} = 1.23 \times 37.05 = 45.57$ p.u., where $\lambda^*_{nor} = 1.23$ is the loading factor value derived from without SVC installation. The load flow when system operating on LM is also shown in Table III. Compared with the base-case load flow, it can be found that most of the voltage magnitudes at the PQ buses are largely decreased due to the increased system load. The largest voltage magnitude decrease is found at bus 6 because of the largely increased demand, while the least voltage magnitude decrease happens at bus 17 due to the sufficient reactive power supply from the connected generators.

Respectively consider each $\mathrm{N}-1$ line outage and calculate the RI value. As a result, when line 11 broken, a converged load flow solution cannot be found due to shortage of power supply since the generator at bus 7 becomes isolated, resulting in the biggest RI value among all outages. Using the biggest RI value as base, the percentages of the RI values for individual line outages are shown in Fig. 5. In the study, except line 11 outage, the line outages with percentages of RI values bigger than 30% are considered for reactive power compensation (i.e., SVC installation), and thus the outages of lines 2, 3, 4, 5, 10, and 26 are

TABLE I
Data for Transmission Lines

Line NO.	From bus	To bus	Impedance p.u. (100MVA base) R	X	B	Failure rate Occ./yr
1	1	2	0.0026	0.0139	0.4611	0.24
2	1	3	0.0546	0.2112	0.0572	0.51
3	1	5	0.0218	0.0845	0.0229	0.33
4	2	4	0.0328	0.1267	0.0343	0.39
5	2	6	0.0479	0.1920	0.0520	0.48
6	3	9	0.0308	0.1190	0.0322	0.38
7	3	24	0.0023	0.0839	0	0.02
8	4	9	0.0268	0.1037	0.0281	0.36
9	5	10	0.0228	0.0883	0.0239	0.34
10	6	10	0.0139	0.0604	2.4590	0.33
11	7	8	0.0159	0.0614	0.0166	0.30
12	8	9	0.0427	0.1651	0.0447	0.44
13	8	10	0.0427	0.1651	0.0447	0.44
14	9	11	0.0023	0.0839	0	0.02
15	9	12	0.0023	0.0839	0	0.02
16	10	11	0.0023	0.0839	0	0.02
17	10	12	0.0023	0.0839	0	0.02
18	11	13	0.0061	0.0476	0.0999	0.40
19	11	14	0.0054	0.0418	0.0879	0.39
20	12	13	0.0061	0.0476	0.0999	0.40
21	12	23	0.0124	0.0966	0.2030	0.52
22	13	23	0.0111	0.0865	0.1818	0.49
23	14	16	0.0050	0.0389	0.0818	0.38
24	15	16	0.0022	0.0173	0.0364	0.33
25(*2)	15	21	0.0063	0.0490	0.1030	0.41
26	15	24	0.0067	0.0519	0.1091	0.41
27	16	17	0.0033	0.0259	0.0545	0.35
28	16	19	0.0030	0.0231	0.0485	0.34
29	17	18	0.0018	0.0144	0.0303	0.32
30	17	22	0.0135	0.1053	0.3312	0.54
31(*2)	18	21	0.0033	0.0259	0.0545	0.35
32(*2)	19	20	0.0051	0.0396	0.0833	0.38
33(*2)	20	23	0.0028	0.0216	0.0455	0.34
34	21	22	0.0087	0.0678	0.1424	0.45

TABLE II
Base Load and Power Supplies

Bus	P_G	P_D	Q_D
1	2.37	1.40	0.29
2	2.37	1.26	0.26
3	-	2.34	0.48
4	-	0.96	0.20
5	-	0.92	0.18
6	-	1.77	0.36
7	3.71	1.63	0.33
8	-	2.22	0.46
9	-	2.28	0.47
10	-	2.54	0.52
11	-	-	-
12	-	-	-
13*	7.30	3.45	0.70
14	-	2.52	0.51
15	0.89	4.12	0.83
16	1.91	1.30	0.26
17	-	-	-
18	4.94	4.33	0.88
19	-	2.35	0.48
20	-	1.66	0.34
21	4.94	-	-
22	3.71	-	-
23	8.15	-	-
24	-	-	-
Total	40.29	37.05	7.54

TABLE III
LOAD FLOWS ON BASE-CASE AND WHEN OPERATING ON LM

Bus	Base-Case				Operating on LM			
	Mag.	Ang.	MW	MVAR	Mag.	Ang.	MW	MVAR
1	1.0350	-0.1958	0.9672	0.2037	1.0350	-0.1556	9.9935	3.2492
2	1.0350	-0.1967	1.1102	-0.0732	1.0350	-0.2153	0.6848	4.8596
3	0.9513	-0.2040	-2.3400	-0.4810	0.6538	-0.6476	-5.2238	-1.0738
4	0.9723	-0.2541	-0.9620	-0.1950	0.7664	-0.5424	-2.1476	- 0.4353
5	1.0100	-0.2544	-0.9230	-0.1820	0.7928	-0.4608	-2.0606	- 0.4063
6	1.0459	-0.3163	-1.7680	-0.3640	0.6147	-0.8742	-3.9452	- 0.8123
7	1.0250	-0.1150	2.0800	0.4578	1.0250	-0.0556	6.3603	4.5584
8	0.9719	-0.2360	-2.2230	-0.4550	0.7227	-0.4992	-4.9627	- 1.0158
9	0.9678	-0.2030	-2.2750	-0.4680	0.7231	-0.5371	-5.0787	- 1.0447
10	1.0205	-0.2409	-2.5350	-0.5200	0.7006	-0.6138	-5.6593	- 1.1604
11	0.9891	-0.0898	0.0000	0.0000	0.8605	-0.1469	0.0000	0.0000
12	0.9989	0.0621	0.0000	0.0000	0.8470	-0.1745	0.0000	0.0000
13	1.0200	0.0000	1.3224	0.6860	1.0200	0.0000	6.0135	6.2941
14	0.9800	-0.0377	-2.5220	-0.6081	0.9800	-0.0006	1.6259	1.8408
15	1.0140	0.1068	-3.2318	-0.0954	1.0140	0.0353	-5.1854	3.4496
16	1.0170	0.1057	0.6142	0.4563	1.0170	0.0604	3.0247	1.0123
17	1.0384	0.1921	0.0000	0.0000	1.0365	0.1561	0.0000	0.0000
18	1.0500	0.2166	0.6110	0.7708	1.0500	0.1727	-0.6999	1.0791
19	1.0185	0.0953	-2.3530	-0.4810	1.0003	-0.0239	-5.2530	- 1.0738
20	1.0347	0.1297	-1.6640	-0.3380	1.0232	0.0034	-3.7148	- 0.7546
21	1.0500	0.2323	4.9400	1.2650	1.0500	0.1974	5.8051	1.6601
22	1.0500	0.3568	3.7050	-0.3551	1.0500	0.4165	6.2045	- 0.1856
23	1.0500	0.1640	8.1510	1.6293	1.0500	0.0540	8.3642	4.2534
24	0.9733	-0.0058	0.0000	0.0000	0.8242	-0.1435	0.0000	0.0000

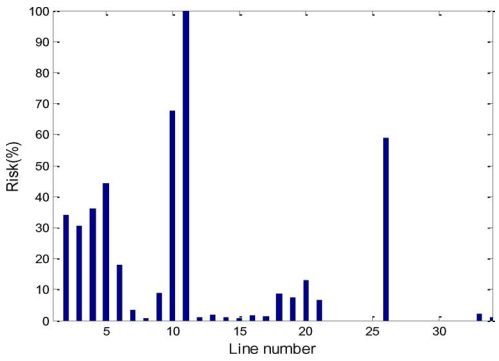

Fig. 5. Percentages of RI values for various N − 1 line outages.

TABLE IV
CF VALUES OF BUSES NECESSARY FOR SVC INSTALLATION UNDER N − 1 LINE OUTAGES WITH HIGH RI VALUES

Outage	Line 2	Line 3	Line 4	Line 5	Line 10	Line 26
$\Delta\lambda_{Ei}$	0.32	0.42	0.43	0.44	0.93	0.67
CF	Bus 3/0.18	Bus 5/0.29	Bus 4/0.30	Bus 6/0.23	Bus 6/0.59	Bus 24/0.44
	Bus 6/0.14	Bus 6/0.19	Bus 9/0.17	Bus 10/0.16	Bus 3/0.13	Bus 3/0.34
	Bus 4/0.13	Bus 10/0.18	Bus 3/0.15	Bus 3/0.13	Bus 4/0.12	Bus 6/0.16
Sel.	Buses 3, 4, 5, 6					

involved in the following analysis. The decreased LM under the six line outages represented as $\Delta\lambda_{E_i}\ \forall i \in \{2,3,4,5,10,26\}$ can be found in Table IV. Since the impact from line 11 outage is so serious that there is no converged load flow solution, in the study, it is suggested to build a parallel line.

Table IV also shows the three buses with first biggest CF values obtained from the application of MA technique to each of the six line outages. For example, the CF value on bus 3 due to line 2 outage is 0.18, expressed as Bus 3/0.18, shown in the second column of Table IV. Since the decreased LM represents the serious degree that an outage would strike against the system, as line 10 broken, $\Delta\lambda_{E_{10}} = 0.93$ being the biggest decreased LM and thus buses 3, 4, and 6 will be responsible for the biggest impact of voltage decrease. These three buses are first selected for SVC installation. It can be found from Table IV that,

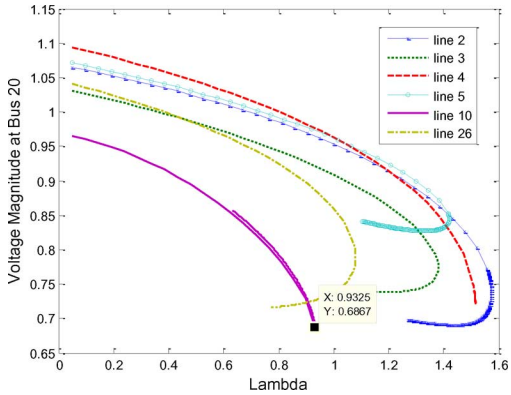

Fig. 6. Under various line outages the P-V curves at bus 20 due to an SVC installation at buses 3, 4, 5, and 6, respectively.

in the three buses specified for SVC installation, at least two buses are also incorporated in the buses with biggest CF values for the other considered line outages but line 3 outage. Through several simple tests, bus 5 with the biggest CF value for line 3 outage is also identified to be necessary for SVC installation because only with the additional SVC installation the required LM ($\lambda_E^* \geq 0.93$) can be achieved when line 3 outage occurs. Then, under each line outage, buses 3, 4, 5, and 6 are, respectively, installed with an SVC, each with 3 p.u. reactive power, and obtained from CPF analysis the P-V curves as well as the LM are shown in Fig. 6. As seen in Fig. 6, among the considered outages, the smallest LM is found at $\lambda_{E_{10}}^* = 0.93$ when line 10 outage, resulting in $\Delta\lambda_{E_{10}} = \lambda_{nor}^* - \lambda_{E_{10}}^* = 1.23 - 0.93 = 0.3$, which is much smaller than 0.93 before SVC installation. Therefore, it is shown that, through the SVC installation, system LM can be improved up close to the level before the outages happen and thus buses 3, 4, 5, and 6 are considered to be suitable for making an optimal SVC installation in the following study.

Under each considered line outage, respectively, installing an SVC at buses 3, 4, 5, and 6, each SVC with 3 p.u. reactive power as the capacity limit, the MOPSO method with 30 particles is used to solve the multi-objective optimal SVC installation problem. The number of nondominated solutions in the Pareto front set for each outage condition is set to 100 and the iterations for deriving a Pareto front set is set to 5000. From the Pareto front sets obtained, the objective functions values f_1 versus f_2 are shown with curves in Fig. 7. For an example representing $\lambda_E^* = 0.8$ as the required LM, it can be seen from Fig. 7 that the SVC installations for line 10 outage requires the highest installation cost; the next higher SVC installation costs in descending order are for lines 26, 3, 5, and 4 outages, and the minimum SVC installation cost is for line 2 outage. Therefore, due to cost-effectiveness consideration, the results of the SVC installations for line 10 outage are taken as the basis to seek for the optimal SVC installation under all considered line outages. Observing the curve from the Pareto front set for line 10 outage, it can be seen that the maximum LM (f_1) is $\lambda_{E_{10}}^* = 0.93$ and, from the solutions in the Pareto front set with $\lambda_{E_{10}}^* = 0.93$, the minimum SVC installation cost (f_2) is found to be 444.6 (US$/h).

If $\lambda_{E_i}^* \geq 0.93$ is required for the LM enhancement, by applying performance index f_1/f_2 to the results for each consid-

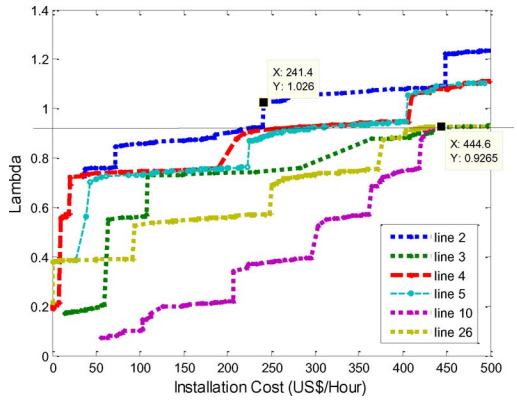

Fig. 7. Curves of the objective functions values f_1 versus f_2 from the Pareto front sets for all considered $\mathrm{N}-1$ outages.

TABLE V
RESULTS OF SVC INSTALLATIONS WITH BIGGEST PERFORMANCE INDEX VALUES FOR ALL CONSIDERED LINE OUTAGES

Outage Line		2	3	4	5	10	26	Sch.
f_1		1.0	0.93	0.93	0.93	0.93	0.93	0.93
f_2		241.4	473.8	282.5	331.5	444.6	431.5	1317.7
Bus	3	0.87	0.22	0.13	0.05	0.02	2.94	2.94
(p.u.)	4	0.05	0.15	0.88	0.12	0.02	0.01	0.88
	5	0.04	1.16	0.06	0.06	0.01	0.01	1.16
	6	0.03	0.45	0.08	1.24	2.98	0.00	2.98

ered line outage, the solution with $\lambda^*_{E_i} \geq 0.93$ in the respective Pareto front sets and with maximum performance index value is shown in Table V. Also, derived from the union of all SVC installation results shown in columns 2 to 7, the SVC installation scheme recommended for LM enhancement in the study is also shown in the last column. As can be seen, in order for the SVC installation scheme to cope with all $\mathrm{N}-1$ line outages, the capacities for the respective SVC installations at the four specified buses should be the biggest settings among those for all considered outages, and thus the operating cost $f_2 = 1317.7$ (US$/h) would be much bigger than that for each outage. The capacities of the SVC installations at buses 3, 4, 5, and 6 are 2.94 p.u., 0.88 p.u., 1.16 p.u., and 2.98 p.u., respectively. The recommended SVC installation scheme is then considered as the optimal SVC installation that can maintain LM at when outage occurs at one line but line 11. As mentioned above, it is suggested to build a parallel line with line 11.

B. Taiwan Power System

The simplified Taipower 345-kV transmission network with 76 buses, including 50 PQ buses, 25 PV buses, and 113 transmission lines, is also used for testing. The network is divided into three areas: north, central, and south areas. One line diagram of the central part of the studied EHV system is shown in Fig. 8. The system demand and supply during peak-load hours are shown in Table VI. Demand in the north area is higher than those in the central and south areas. For most of the time, the north has to count on the support from the south. Load increments ΔP_{Di} and ΔQ_{Di} for each PQ bus i are set to 10 percent

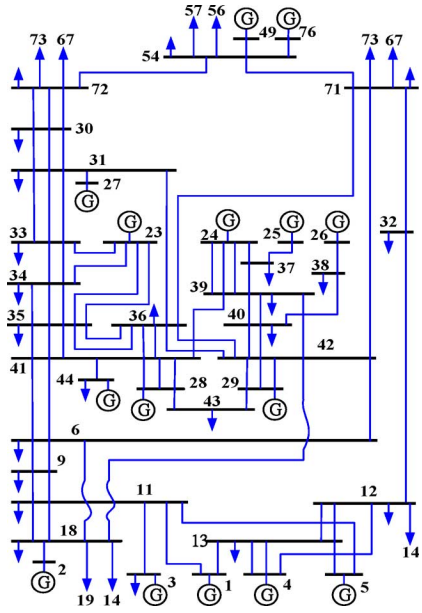

Fig. 8. Central part of Taipower network.

TABLE VI
SUPPLY AND DEMAND AT DIFFERENT AREAS, AND STUDIED CONTINGENCY SCENARIOS AND COMPUTED LOADING MARGINS

Area (Bus)		North (45-76)	Central (23-44)	South (1-22)	Total x100MW
Gen. Capacity		205.22	134.56	161.63	501.41
Generation		205.11	118.44	124.43	447.98
Demand		196.09	122.76	126.03	444.89
Contingency		Scenario			λ^*_E
N-2	1	36-41(CKT 1), 36-42(CKT 1)			0.86
	2	36-41(CKT 1, 2)			0.93
	3	23-33, 33-34(CKT 1)			0.91
N-2G-1*	4	36-42(CKT 1)			0.84

MVA base = 100MVA
* Two generators in the north area with capacity of 1190.6 MW are out in the N-2G-1 scenario.

base load. The LM at $\lambda^*_{Ei}\ \forall i \in \{1,2,3,4\}$, computed under the four contingency scenarios with biggest RI values before making reinforcement, are also shown in Table VI.

Derived from the application of MA technique, the five buses with biggest CF values for each considered contingency are shown in Table VII. It can be seen that the largest decreased LM is found when contingency 4 happens, calculated as $\Delta\lambda_{E_4} = \lambda^*_{nor} - \lambda^*_{E_4} = 1.12 - 0.84 = 0.28$. In case that the worst contingency scenario is considered to be most essential to cope with for the LM enhancement, buses 30, 31, 32, 71, and 72 with biggest CF values for contingency 4 are then specified for SVC installation. It can be found from Table VII that most of the five buses are also incorporated in the buses with biggest CF values for the other contingencies. Then, under each considered contingency, respectively, installing an SVC with 3 p.u. reactive power at each of the five buses and using the CPF procedure to solve for the LM, it can be found from the derived P-V curves shown in Fig. 9 that $\lambda^*_{Ei} \geq 0.98\ \forall i$. Let the LM of the power system under all considered contingencies be required at $\lambda^*_E \geq 0.97$,

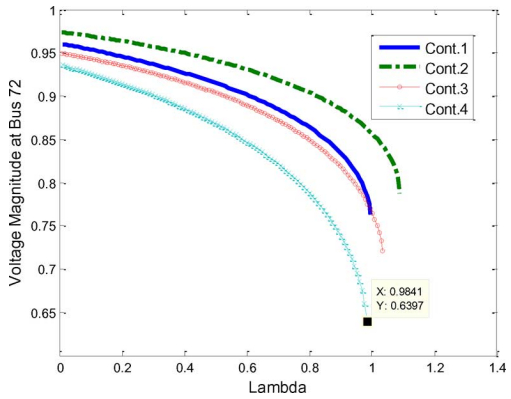

Fig. 9. Under all considered contingency scenarios the P-V curves at bus 72 due to an SVC installation at buses 30, 31, 32, 71, and 72, respectively.

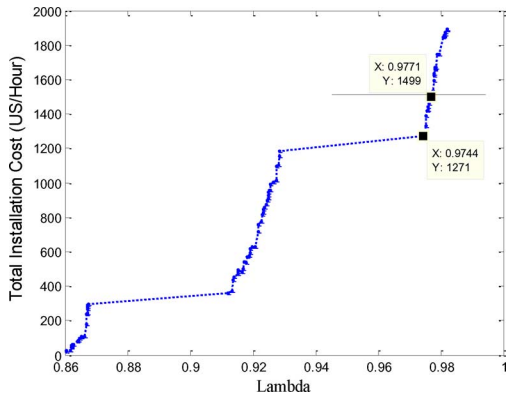

Fig. 11. Various LM versus the corresponding installation costs for different SVC installation schemes.

TABLE VII
CF VALUES OF BUSES NECESSARY FOR SVC INSTALLATION UNDER CONTINGENCIES WITH HIGH RI VALUES

Contingency	1	2	3	4
$\Delta\lambda_{Ei}$	0.26	0.19	0.21	0.28
CF	Bus 32/0.63	Bus 32/0.61	Bus 30/0.57	Bus 32/0.53
	Bus 36/0.46	Bus 31/0.35	Bus 33/0.32	Bus 30/0.17
	Bus 30/0.27	Bus 30/0.34	Bus 36/0.27	Bus 31/0.16
	Bus 31/0.25	Bus 36/0.33	Bus 31/0.22	Bus 72/0.15
	Bus 71/0.24	Bus 71/0.31	Bus 32/0.20	Bus 71/0.14
Sel.	Buses 30, 31, 32, 71, 72			

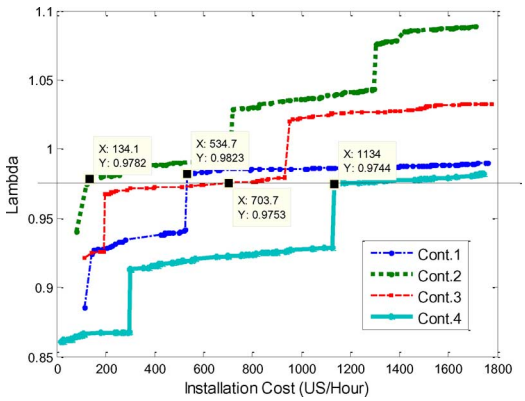

Fig. 10. Curves of the objective functions values f_1 versus f_2 from the Pareto front sets for all considered contingencies.

TABLE VIII
RESULTS OF SVC INSTALLATIONS WITH BIGGEST PERFORMANCE INDEX VALUES FOR ALL CONSIDERED CONTINGENCIES

Contingency		1	2	3	4	Sch.
f_1		0.98	0.98	0.98	0.97	0.97
f_2		534.7	134.1	703.7	1134	1271
Bus (p.u.)	30	0.96	0.17	1.31	0.96	1.31
	31	0.19	0.07	0.77	2.06	2.06
	32	2.00	0.07	0.18	2.83	2.83
	71	0.28	0.05	0.28	0.44	0.44
	72	0.47	0.12	0.44	0.05	0.47

and it will be feasible to make an optimal SVC installation at the five buses.

Using 3 p.u. reactive power as the capacity limit for each SVC installation, the MOP under each considered contingency is solved by the MOPSO algorithm with 30 particles and 5000 iterations to derive a Pareto front set with the number of nondominated solutions set to 100. The curves of the objective functions values f_1 versus f_2 from the Pareto front sets for all considered contingencies are shown in Fig. 10. By using the proposed LM enhancement strategy in Fig. 2, the curve of the LM versus the corresponding SVC installation costs for different SVC installation schemes is shown in Fig. 11. As can be found from Fig. 11 that the LM obtained with an SVC installation scheme will be at one value of λ_E^* between 0.86 and 0.98 corresponding to an SVC installation cost between 19.0 US$/h and 1889 US$/h. Let 1500 US$/h be the allowable investment cost for SVC installation and the required LM be at $\lambda_E^* \geq 0.97$. Eventually, the results of the optimal SVC installation scheme derived from the union of the solutions for all considered contingencies, i.e., from Fig. 11, are shown in the last column of Table VIII. As seen that the scheme suggested has LM at $\lambda_E^* = 0.974$ and the SVC installation cost is 1271 US$/h which is less than the allowable investment cost. On the other hand, if an SVC installation scheme with LM at $\lambda_E^* > 0.9771$ is selected, as can be seen in Fig. 11 that, although the LM is larger than that ($\lambda_E^* = 0.9744$) obtained with the scheme suggested, obviously the economic constraint, representing the allowable investment cost, is violated since the SVC installation cost is bigger than 1500 US$/h.

V. CONCLUSION

From a long-term economic development point of view, it is expectable that regional or integral electric power demands will increase or change constantly. Besides, in the deregulated electrical power systems, due to open access to the transmission networks, various types and a large amount of power transactions would result in huge changing power flow. In this view, serious threats to power system operation security might occur. To improve the operation security of power systems while avoiding network expansion by building more transmission lines, it is a good choice to suitably install FACTS devices in existing networks such that they can accommodate more power transfer. The MOP proposed in the paper considering the most serious contingencies to seek a Pareto front set for each contingency is solved by using the fitness sharing MOPSO method. The proposed performance index is then used to determine an optimal

SVC installation scheme for the required LM with the SVC installation locations and capacities derived from the union of the SVC installations for all considered contingencies. From the test results, the achievement of the proposed strategy for SVC installation, that is well consistent with specific economic and technical concerns, is validated.

REFERENCES

[1] A. X. Chen, L. Z. Zhang, and J. Shu, "Congestion management based on particle swarm optimization," in *Proc. 7th Int, Power Engineering Conf. (IPEC 2005)*, vol. 2, pp. 1019–1023.

[2] R. S. Fang and A. K. David, "Transmission congestion management in an electricity market," *IEEE Trans. Power Syst.*, vol. 14, no. 3, pp. 877–883, Aug. 1999.

[3] A. A. Athamneh and W. J. Lee, "Benefits of FACTS devices for power exchange among Jordanian interconnection with other countries," in *Proc. IEEE PES General Meeting*, Jun. 2006.

[4] Blackout of 2003: Description and Responses. [Online]. Available: http://www.pserc.wisc.edu/.

[5] A. Sode-Yome, N. Mithulananthan, and K. Y. Lee, "A maximizing loading margin method for static voltage stability in power system," *IEEE Trans. Power Syst.*, vol. 21, no. 2, pp. 799–808, May 2006.

[6] A. Sode-Yome and N. Mithulananthan, "An economical generation direction for power system static voltage stability," *Elect. Power Syst. Res.*, vol. 76, no. 12, pp. 1075–1083, Aug. 2006.

[7] M. M. Farsangi, H. Nezamabadi-pour, Y. H. Song, and K. Y. Lee, "Placement of SVCs and selection of stabilizing signals in power systems," *IEEE Trans. Power Syst.*, vol. 22, no. 3, pp. 1061–1071, Aug. 2007.

[8] S. Gerbex, R. Cherkaoui, and A. J. Germond, "Optimal location of multi-type FACTS devices in a power system by means of genetic algorithms," *IEEE Trans. Power Syst.*, vol. 16, no. 3, pp. 537–544, Aug. 2001.

[9] K. Y. Lee, M. M. Farsangi, and H. Nezamabadi-pour, "Hybrid of analytical and heuristic techniques for FACTS devices in transmission systems," in *Proc. IEEE PES General Meeting*, Jun. 2007, pp. 1–8.

[10] A. R. Messina, M. A. Pérez, and E. Hernández, "Co-ordinated application of FACTS devices to enhance steady-state voltage stability," *Int. J. Elect. Power Energy Syst.*, vol. 25, no. 4, pp. 259–267, 2003.

[11] A. Sode-Yome, N. Mithulananthan, and K. Y. Lee, "A comprehensive comparison of FACTS devices for enhancing static voltage stability," in *Proc. IEEE PES General Meeting*, Jun. 2007, pp. 1–8.

[12] M. Jáfari and S. Afsharnia, "Voltage stability enhancement in contingency condition using shunt FACTS devices," in *Proc. Int. Conf. "Computer as Tool" (EUROCON 2007)*, Sep. 2007, pp. 9–12.

[13] L. J. Cai, I. Erlich, and G. Stamtsis, "Optimal choice and allocation of FACTS devices in deregulated electricity market using genetic algorithms," in *Proc. 2004 IEEE/PES Power Systems Conf. Expo.*, pp. 201–207.

[14] T. S. Chung and Y. Z. Li, "A hybrid GA approach for OPF with consideration of FACTS devices," *IEEE Power Eng. Rev.*, vol. 21, no. 2, pp. 47–50, Feb. 2001.

[15] Y. Matsuo and A. Yokoyama, "Optimization of installation of FACTS devices in power system planning by both tabu search and nonlinear programming methods," in *Proc. 1999 Intelligent System Application to Power System Conf.*, pp. 250–254.

[16] S. N. Singh and A. K. David, "A new approach for placement of FACTS devices in open power markets," *IEEE Power Eng. Rev.*, vol. 21, no. 9, pp. 58–60, Sep. 2001.

[17] P. Bhasaputra and W. Ongsakul, "Optimal power flow with multi-type of FACTS devices by hybrid TS/SA approach," in *Proc. IEEE Int. Conf. Industrial Technology*, Dec. 2002, vol. 1, pp. 285–290.

[18] H. A. Abdelsalam, G. E. M. Aly, M. Abdelkrim, and K. M. Shebl, "Optimal location of the unified power flow controller in electrical power system," in *Proc. IEEE Large Engineering Systems Conf. Power Engineering*, Jul. 2004, pp. 41–46.

[19] E. N. Azadani, S. H. Hosseinian, M. Janati, and P. Hasanpor, "Optimal placement of multiple STATCOM," in *Proc. 12th Int. Middle-East Power System Conf. (MEPCON 2008)*, Mar. 2008, pp. 523–528.

[20] D. Povh, "Modeling of FACTS in power system studies," in *Proc. IEEE PES Winter Meeting*, Jan. 2000, vol. 2, pp. 1435–1439.

[21] H. R. Baghaee, M. Annati, and B. Vahidi, "Improvement of voltage stability and reduce power system losses by optimal GA-based allocation of multi-type FACTS devices," in *Proc. 11th Int. Conf. Optimization of Electrical and Electronic Equipment (OPTIM 2008)*, May 2008, pp. 209–214.

[22] A. S. Yome, N. Mithulananthan, and K. Y. Lee, "Static voltage stability margin enhancement using STATCOM, TCSC and SSSC," in *Proc. 2005 IEEE/PES Transmission and Distribution Conf. Exhib.*, pp. 1–6.

[23] Z. Lu, M. S. Li, and L. Jiang, "Optimal allocation of FACTS devices with multiple objectives achieved by bacterial swarming algorithm," in *Proc. IEEE PES General Meeting—Conversion and Delivery of Electrical Energy in the 21st Century*, Jul. 2008, pp. 1–7.

[24] A. Laífa and M. Boudour, "FACTS allocation for power systems voltage stability enhancement using MOPSO," in *Proc. IEEE 5th Int. Multi-Conf. Systems, Signals and Devices (IEEE SSD 2008)*, Jul. 2008, pp. 1–6.

[25] S. L. Maximino and E. R. Jonathan, "Particle swarm optimization and fitness sharing to solve multi-objective optimization problems," in *Proc. Congr. Evolutionary Computation (CEC 2005)*, Sep. 2005, pp. 1204–1211.

[26] C. A. C. Coello, G. T. Pulido, and S. L. Maximino, "Handling multiple objectives with particle swarm optimization," *IEEE Trans. Evol. Computat.*, vol. 8, no. 3, pp. 256–279, Jun. 2004.

[27] M. Saravanan *et al.*, "Application of PSO technique for optimal location of FACTS devices considering system loadability and cost of installation," in *Proc. Int. Power Engineering Conf. (IPEC 2005)*, Dec. 2005, vol. 2, pp. 716–721.

[28] J. McCalley, A. Fouad, V. Vittal, A. Irizarry-Rivera, B. Agrawal, and R. Farmer, "A risk-based security index for determining operating limits in stability-limited electric power systems," *IEEE Trans. Power Syst.*, vol. 12, no. 3, pp. 1210–1219, Aug. 1997.

Ya-Chin Chang (M'10) received the Ph.D. degree from National Sun Yat-Sen University, Kaohsiung, Taiwan, in 2002.

He is an Associate Professor with the Department of Electrical Engineering, Cheng Shiu University, Kaohsiung, Taiwan. His research interests are in power system operation and planning.